

RESEARCH

Open Access



Influence of sulfide, chloride and dissolved organic matter on mercury adsorption by activated carbon in aqueous system

Chi Chen, Yu Ting, Boon-Lek Ch'ng and Hsing-Cheng Hsi*

Abstract

Using activated carbon (AC) as thin layer capping to reduce mercury (Hg) released from contaminated sediment is a feasible and durable remediation approach. However, several aqueous factors could greatly affect the Hg fate in the aquatic system. This study thus intends to clarify the influences on Hg adsorption by AC with the presence of sulfide, dissolved organic matter (DOM), and chloride. The lab-scale batch experiments were divided into two parts, including understanding (1) AC adsorption performance and (2) Hg distribution in different phases by operational definition method. Results showed that the Hg adsorption rate by AC was various with the presence of sulfide, chloride, and DOM (from fast to slow). Hg adsorption might be directly bonded to AC with Hg-Cl and Hg-DOM complexes and the rate was mainly controlled by intraparticle diffusion. In contrast, "Hg + sulfide" result was better described by pseudo-second order kinetics. The Hg removal efficiency was 92–95% with the presence of 0–400 mM chloride and approximately 65–75% in the "Hg + sulfide" condition. Among the removed Hg, 24–29% was formed into aqueous-phase particles and about 30% Hg was adsorbed on AC with 2–20 μM sulfide. Increasing DOM concentration resulted in more dissolved Hg. The proportion of dissolved Hg increased 31% by increasing DOM concentration from 0.25 to 20 mg C L^{-1} . Simultaneously, the proportion of adsorbed Hg by AC decreased by 47%. Overall, the presence of chloride increases the Hg adsorption by AC. In contrast, the presence of sulfide and DOM causes a negative effect on AC adsorption.

Keywords: Mercury, Activated carbon, Chloride, Sulfide, Dissolved organic matter

Introduction

Mercury (Hg) has been known as one of the most toxic heavy metals to human beings and living organisms [1–3]. Despite the decreasing industrial use of Hg in the past recent years, human activities including fossil fuel combustions, gold-mining, and manufacturing industries have contributed to the increased Hg levels in the atmosphere and aquatic environments [4]. The released Hg could ultimately transport to aquatic system and accumulate in sediment through wet or dry deposition. Thus, the formation and bioaccumulation of methylmercury (MeHg) formed from inorganic Hg under reducing conditions in sediment could put a serious threat to aquatic ecosystems [5, 6].

Several technical challenges still remain to remediate contaminated sediment, as the traditional approaches could not achieve risk reduction goals for human health and ecosystem protection and may even cause secondary pollution [7–9]. For example, dredging followed by ex-situ approaches has been typically used because of its long-term effectiveness and relatively short remediation time [10]. Nevertheless, dredging could be very costly and results into remobilization of contaminants [11]. In-situ thin-layer capping, which involves the use of chemically reactive materials that reduce the mobility, toxicity, and bioavailability of the contaminant, subsequently reducing ecological and human health risk, has been developed as a novel remediation of contaminated sediment [7, 12]. The use of activated adsorbents as capping materials has turned out to be a less expensive and high potential

* Correspondence: hchsi@ntu.edu.tw

Graduate Institute of Environmental Engineering, National Taiwan University, Taipei 10617, Taiwan



© The Author(s). 2020 **Open Access** This article is licensed under a Creative Commons Attribution 4.0 International License, which permits use, sharing, adaptation, distribution and reproduction in any medium or format, as long as you give appropriate credit to the original author(s) and the source, provide a link to the Creative Commons licence, and indicate if changes were made. The images or other third party material in this article are included in the article's Creative Commons licence, unless indicated otherwise in a credit line to the material. If material is not included in the article's Creative Commons licence and your intended use is not permitted by statutory regulation or exceeds the permitted use, you will need to obtain permission directly from the copyright holder. To view a copy of this licence, visit <http://creativecommons.org/licenses/by/4.0/>.

approach due to the ability to adsorb newly deposited contaminants. In previous studies of our research group, activated carbon (AC) was reported to successfully inhibit inorganic Hg and MeHg release into the overlying water in a lab-scale microcosm experiment [13, 14]. AC has been widely known as an effective adsorbent to remove Hg in recent years [15–19].

Several environmental factors, namely sulfide, chloride, and dissolved organic matter (DOM) could significantly affect the Hg fate in aquatic systems. The sulfide minerals in sediment are mainly the products of oxidizing organic matters by sulfate-reducing bacteria [20]. Sulfide has high affinity for Hg and can form HgS particles; the forming of HgS_(s) structure may inhibit Hg from being methylated and being transported [21–23]. Hg²⁺ concentrations are quite low as compared to sulfide concentration in aquatic ecosystems. Therefore, sulfides could control Hg speciation significantly and play an important role for stabilizing Hg in sediment [24].

Natural DOM in the stream water is typically at the range of 1 to 5 mg C L⁻¹, while in some high-organic soils or vegetated environments, DOM may have concentrations up to 20 or 50 mg C L⁻¹ [25]. DOM is shown to hinder the aggregation of HgS particles by forming coordinate covalent bonds between functional groups on the organic molecules and atoms on the surface of the particles [26]. Importantly, Hg interacted with DOM increased the methylating rate in comparison to Hg²⁺; moreover, the β-HgS nanoparticles formed by Hg mixed with sulfide and DOM have a higher availability than β-HgS microparticles for bacterial methylation [26]. Recent studies have also shown that thiol functional groups are the major binding sites which mainly increases solubility, mobility and toxicity of Hg [27, 28].

The oxidation and reduction of Hg in the presence of chloride ion (Cl⁻) have also been studied mainly in oxic environments. The Hg-Cl complexes were regarded as non-adsorption Hg speciation in previous studies. Hg-Cl complexes were also reported to inhibit Hg reduction to gaseous Hg [29]. Lee et al. [29] also reported that the increase of Cl⁻ concentration inhibited Hg²⁺ reduction rate as the rate constant ranged from 0.14 to 1.7 h⁻¹ in the presence of Cl⁻ as compared to 2.4 h⁻¹ in the absence of Cl⁻. Consequently, the health risk of organisms in the aquatic ecosystem is dependent on Hg chemical speciation and the phase of Hg rather than total Hg concentrations in the sediments.

Past studies showed that sulfide, DOM, and chloride ions could stabilize Hg in aquatic system. To further inference, sulfide, DOM, and chloride might inhibit Hg adsorption by AC and influence the Hg partitioning within various phases (i.e., aqueous, AC, and precipitation phases) that are still needed to be better comprehended. Therefore, in this study, batch experiments were conducted to gain further knowledge on the behavior of Hg

adsorption by AC affected by sulfide, DOM, and chloride at various concentrations. The results obtained from this work could help clarifying the Hg adsorption mechanism by AC under the presence of essential elements in natural habitat, especially focusing on the impacts of sulfide, DOM, and chloride, and further help justifying whether thin layer capping can be applied to the aquatic system with the presence of these compounds at various concentrations.

Materials and methods

Lab-scale batch experiments were conducted to better understand the influences of sulfide, chloride, and DOM concentrations on Hg adsorption equilibrium and kinetics of AC in an aqueous system. The characterization of AC was also conducted to comprehend the effects of physicochemical properties of AC on Hg adsorption.

Physicochemical properties of AC

Commercial granular activated carbon (Wel Han Environmental Industrial Co., Taiwan) prepared from high-quality coconut shell was used. The AC was first washed with deionized water to remove fine particle and impurity, then dried at 60 °C in a drying oven for 24 h. After cooling in the drying oven, the AC was sieved by 10–18 mesh (1–2 mm) standard screens and stored for subsequent tests.

The specific surface area (S_{BET}), total pore volume (V_{total}), and micropore surface area (S_{micro}) and micropore surface area (V_{micro}) of AC were determined by N₂ adsorption isotherm at 77 K (Micromeritics ASAP 2020). Brunauer–Emmett–Teller (BET) method was applied to evaluate S_{BET} , V_{total} was calculated by total N₂ volume adsorbed by AC at the relative pressure near one. The t-plot method was applied to evaluate the micropore volume and micropore surface area. Non-local density functional theory (NLDFT) model was applied to evaluate the pore size distribution of micropore. Barrett–Joyner–Halenda method was used to evaluate the pore size distribution of mesopore and macropore.

The morphology of AC samples was studied by scanning electron microscopy (SEM: JOEL JSM-7500F) with an accelerating voltage of 15 kV. AC was coated with a thin layer of gold to increase their electrical conductivity and stability, so that they can withstand the high vacuum conditions during analysis.

The elemental analyses were conducted to measure the contents of elements including nitrogen, carbon, hydrogen, sulfur (Vario EL cube, Elementar), and oxygen (Flash 2000, Thermo Fisher).

The zeta potential of AC under different pHs (1–9) was determined (Malvern Zetasizer Nano Z analyzer). AC was grounded into small powder for suspension in solution. Samples were prepared by adding 5 mg of AC in 9 mL Milli-Q water and adjusted to a given pH with

NaOH and HNO₃. The total solution volume was around 10 mL for analysis.

X-ray photoelectron spectroscopy (XPS; ULVAC PHI-5000) was conducted with Al K α radiation of 15 kV to comprehend the functional groups on the surface of AC. The binding energies of peaks were referenced to C1s peak at 285 eV.

Batch experiments of Hg adsorption

The batch experiments include two parts: AC adsorption performance tests and Hg distribution tests. The AC adsorption performance experiments include AC dosage test and adsorption kinetic test. The AC dosage test was carried out by adding given amounts of AC into the spiked Hg solution in the absence of chloride, sulfide, and DOM. The adsorption kinetic test and Hg distribution test were carried out by using spiked Hg solution containing various concentrations of chloride, sulfide, and DOM individually under a fixed dosage of AC. The AC adsorption experiments in Hg-spiked solution mixed with chloride, sulfide, and DOM were designated as “Hg + Cl”, “Hg + sulfide”, and “Hg + DOM” respectively in this study. Each experiment was performed in triplicate. The main parameters are listed in Table S1 of Supplemental Materials.

Preliminary work of solution preparation

All solutions and reagents were prepared in degassed Milli-Q water, which was deoxygenated by purging with high-purity N₂ at least 40 min (oxygen concentration < 2 mg L⁻¹). The Hg²⁺ solutions were prepared by diluting Hg (NO₃)₂ standard solution to 20–40 $\mu\text{g L}^{-1}$ then adding 5 mM sodium nitrate to maintain the ionic strength. Chloride stock solutions were prepared by dissolving sodium chloride in Milli-Q water. Sulfide stock solutions (pH = 11.5 \pm 0.5) were prepared by dissolving crystals of Na₂S·9H₂O in Milli-Q water containing 10 mM H₃BO₃ then used immediately. The concentrations of chloride stock and sulfide stock were determined by UV-Vis spectrophotometer (Merck Spectroquant® Prove 300). DOM stock solutions were prepared by dissolving Suwanee River Humic Acid (SRHA) powder in Milli-Q water. The pH of the DOM stock was adjusted with 0.01 M NaOH to pH 6 then filtered through a 0.2 μm filter and stored in a refrigerator at 4 °C until measuring the total dissolved organic carbon (DOC) with a total organic carbon (TOC) analyzer.

AC adsorption performance

The experimental process followed the steps below:

Preparation of Hg solution The Hg stock was diluted to 20 $\mu\text{g L}^{-1}$ for AC dosage test. The “Hg + Cl” test was carried out by diluting Hg and chloride stock solution to 20 $\mu\text{g L}^{-1}$ and 200 mM respectively in a 1 L beaker. The

“Hg + DOM” test was carried out by diluting Hg and DOM stock solution to 20 $\mu\text{g L}^{-1}$ and 2 mg C L⁻¹ in a 1 L beaker, respectively. The “Hg + sulfide” test was carried out by diluting Hg and sulfide stock solution to 40 $\mu\text{g L}^{-1}$ and 20 μM in each 500 mL beaker, respectively. Then, the sample solution was prepared by mixing equal volume of Hg and sulfide solution. Each Hg sample solution was adjusted to pH 7 \pm 0.5 by using 0.01 M NaOH and 0.01 M HNO₃ before adding AC.

Sample preparation The Hg sample solution was separated in a 50 mL volumetric flask and injected into a 50 mL glass vessel. The intended dosage of AC was added into glass vessels, which were then covered with a rubber stopper and aluminum cap. All of the glass vessels were then coated with aluminum foil to avoid light effect.

Adsorption condition The samples were put into a water-bath incubating shaker and shaken at 125 rpm for 30–2880 min at 30 °C.

Sample analysis For the AC dosage and “Hg + Cl” test, 20 mL of the unfiltered initial Hg sample solution and 5 mL of the solution which was filtered with 0.2 μm filter after AC adsorption were preserved and digestion with 0.5% BrCl at least 1 day before the total Hg concentration (THg) analysis. For “Hg + sulfide” and “Hg + DOM” tests, 20 mL of the initial Hg sample solution and 5 mL of the solution which was filtered with 0.2 μm filter after AC adsorption were preserved with 0.5% BrCl and stored in a refrigerator at 4 °C until microwave digestion by HCl mixed with HNO₃ (3:1 v/v). All the water samples were analyzed for the THg by the cold vapor atomic fluorescence spectrophotometer (CVAFS: Brooks Rand Model 3). The aqueous Hg removal efficiency by AC was calculated by Eq. (1) and the adsorption capacity of AC was calculated by Eq. (2).

$$R(\%) = \frac{C_0 - C_t}{C_0} \times 100\% \quad (1)$$

$$q_e(\mu\text{g g}^{-1}) = \frac{(C_0 - C_t) \times V}{W_{AC}} \quad (2)$$

where R (%) is the Hg removal efficiency, q_e ($\mu\text{g g}^{-1}$) is the adsorption capacity of AC, C_0 ($\mu\text{g L}^{-1}$) is the initial Hg concentration, C_t ($\mu\text{g L}^{-1}$) is the residual Hg concentration at given time, V (L) is the volume of Hg sample solution, and W_{AC} (mg) is the dosage of AC.

To determine the optimum AC dosage for the batch experiments, AC dosage tests were carried out by adding 20, 50, and 80 mg AC in 50 mL Hg solution (20 $\mu\text{g L}^{-1}$). The contact time of AC in “Hg + sulfide” test was controlled at 30, 60, 300, 600, and 1200 min. The contact time of AC in “Hg + Cl” and “Hg + DOM” tests were

controlled at 30, 60, 300, 960, 1440, and 2880 min. The test parameters are listed in [Table S2](#).

Hg distribution test

The purpose of this part of experiment is to realize the Hg distribution, including Hg in dissolved and solid phases under different concentration levels of sulfide/chloride/DOM. The test sample was divided into three parts by operational-defined method included “dissolved Hg”, “particulate Hg”, and “Hg in AC”. The parameters are listed in [Table S3](#). The experimental process was basically the same as the step of AC adsorption performance. The process followed the steps below:

Preparation of Hg solution The “Hg + Cl” and “Hg + DOM” tests were carried out using chloride/DOM solutions containing $20 \mu\text{g L}^{-1}$ Hg in a 1 L beaker. The “Hg + S” test was carried out by mixing the equal volume (500 mL) of different concentrations of sulfide with Hg solution ($40 \mu\text{g L}^{-1}$) to have the solutions containing $20 \mu\text{g L}^{-1}$ Hg. Each Hg solution was adjusted to $\text{pH } 7.0 \pm 0.5$ by 0.01 M NaOH and 0.01 M HNO_3 before adding AC.

Sample preparation The Hg solution was quantitated for 50 mL by volumetric flasks and injected into each glass vessel. The AC was then added into glass vessels and covered with a rubber stopper and aluminum cap. All of the glass vessels were then coated with aluminum foil to avoid light effect.

Adsorption condition The samples were put into a water-bath incubating shaker and shaken at 125 rpm for 1440 min at 30°C .

Sample analysis

(1) Dissolved Hg

The residual Hg in the solution after AC adsorption was defined as “dissolved Hg”. For the “Hg + Cl” test, 5 mL of the solution which was filtered with $0.2 \mu\text{m}$ filter after AC adsorption was preserved and digestion with 0.5% BrCl at least 1 day before THg analysis. For the “Hg + S” and “Hg + DOM” tests, 5 mL of the solution which was filtered with $0.2 \mu\text{m}$ filter after AC adsorption was preserved with 0.5% BrCl and stored in a refrigerator at 4°C until microwave digestion by HCl mixed with HNO_3 (3:1 v/v). All the water samples were analyzed for THg by CVAFS.

(2) Particulate Hg

The particles formed by Hg interacted with sulfide or DOM were defined as “particulate Hg”. The residual

solution was filtered by $0.2 \mu\text{m}$ cellulose acetate membrane filter to intercept the particulate Hg. The membrane filter was preserved in a centrifuge tube and stored at -20°C . Then, freeze dryer system was used to remove moisture. The dried particulate Hg sample was microwave digested by HCl mixed with HNO_3 (3:1 v/v). The samples were estimated for Hg by CVAFS.

(3) Hg in AC

AC collected by manual screening after adsorption was defined as “Hg in AC”. After the residual solution was filtered by $0.2 \mu\text{m}$ cellulose acetate membrane filter and rinsing the glass vessel with Milli-Q water, the AC sample was collected by manual screening and stored at -20°C . Then, freeze dryer system was used to remove moisture. The AC sample was microwave digested by HCl mixed with HNO_3 (3:1 v/v). The samples were estimated for Hg by CVAFS and the actual q_e of AC was subsequently determined.

Sample analysis

The THg in the aqueous sample was determined by CVAFS. The method detection limit of CVAFS used in this study is 0.26 ng L^{-1} . TOC in the water sample is oxidized to form CO_2 , which is then measured by a detection system (Aurora 1030w). The sulfide and chloride analyses were done by test kits and measured in the photometer (Merck Spectroquant® Prove 300). Detailed descriptions pertaining to the analyses of THg, TOC, sulfide, and chloride can be found in the [Supplementary Materials](#).

Results and discussion

Physical and chemical properties of AC

[Table 1](#) shows the physical and chemical properties of AC. The S_{BET} and S_{micro} were 818 and $769 \text{ m}^2 \text{ g}^{-1}$, respectively, and the microporosity (i.e., $V_{\text{micro}}/V_{\text{total}}$) was calculated to be 0.868, indicating that the AC used in this study is highly microporous (pore $< 2 \text{ nm}$). This result is also supported by the pore size distribution based on NLDFT method ([Fig. 1](#)). SEM images of AC also showed that the AC used are particles with sizes around 1–1.5 μm with significant surface roughness that may increase the macropore and surface defects. As a result, without any surface modification process, the AC used retained a well-developed pore structure and distribution that could be beneficial for Hg adsorption. It is worth noting that the presence of micropores is essential for the Hg adsorption; the micropore surface area or volume, however, does not appear to be the only property that affects the Hg adsorption effectiveness [[30](#)]. The presence of active sites, such as oxygenated functional groups in activated carbon, also governs the Hg adsorption.

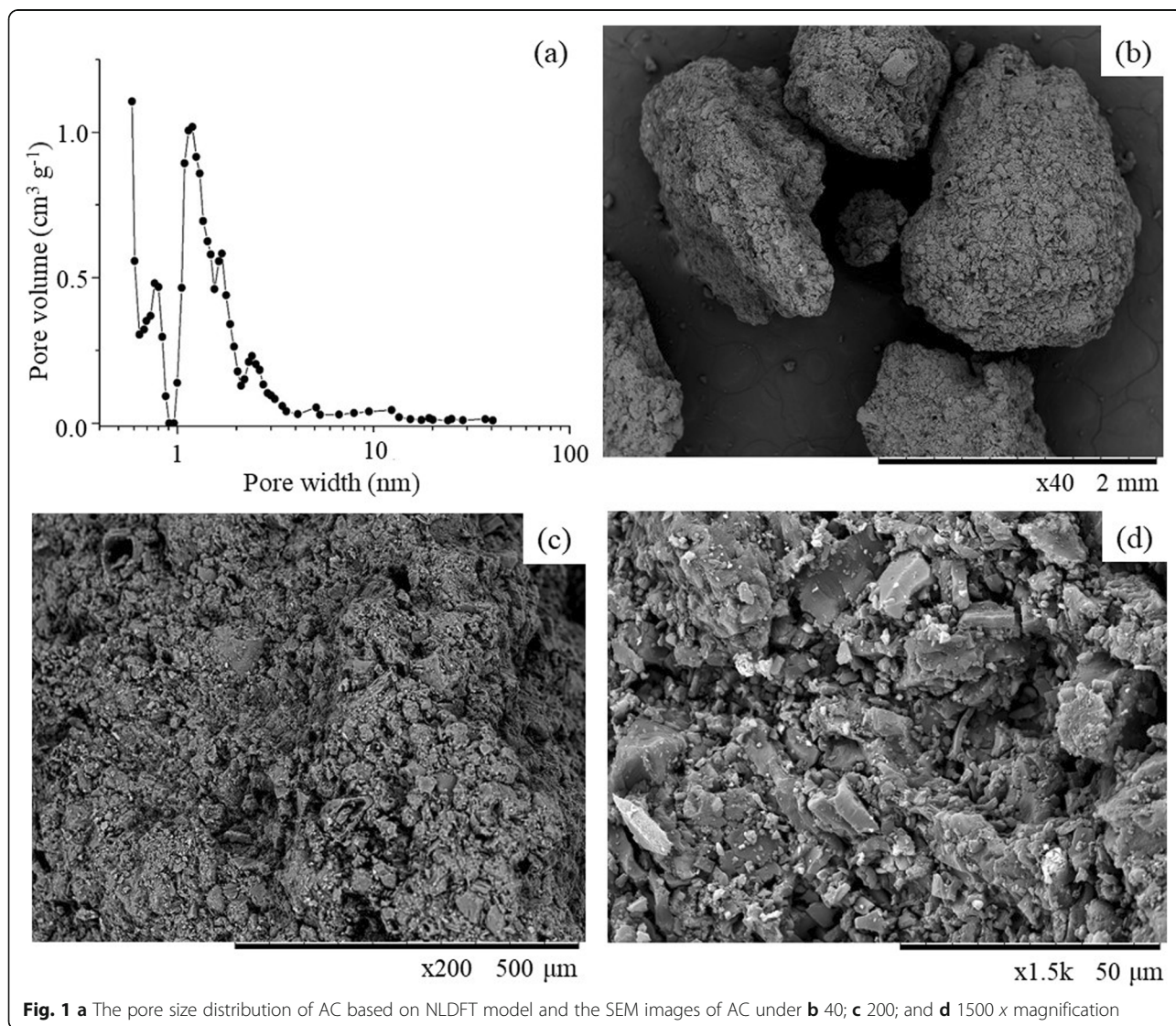
Table 1 The physicochemical properties of AC

S_{BET} ($m^2 g^{-1}$)	S_{micro} ($m^2 g^{-1}$)	V_{total} ($cm^3 g^{-1}$)	V_{micro} ($cm^3 g^{-1}$)	C (wt%)	H (wt%)	O (wt%)	N (wt%)	S (wt%)
818	769	0.462	0.401	78.9	1.41	4.52	0.73	0.47

AC was mainly composed of 78.9 wt% C, 4.52 wt% O, 1.41 wt% H, and 0.73 wt% N (Table 1). There was also a minor content of sulfur (0.47 wt%) in AC, however, it was not apparently existed as a functional group to adsorb Hg as shown in XPS because the peak intensity of S2p was weak (Fig. 2). XPS spectra of AC include (a) wide scan, (b) deconvoluted C1s, and (c) the deconvoluted O1s. The C1s spectra of AC in Fig. 2b could be deconvoluted into four peaks at the binding energies of 284.6, 286.0, 287.6, and 290.4 eV, corresponded to C-C, C-OH, C=O and COOH, respectively, according to Martinez et al. [31]. The O1s spectra of AC in Fig. 2c was deconvoluted into six peaks at the binding energies of 530.2, 531.1, 531.8, 532.5, 533.4,

534.5, and 538.4 eV, corresponded to quinone, COOH, C=O, C-O, C-OH, and chemisorbed oxygen, respectively [32]. The test AC contained numerous oxygen functional groups, which were well known as effective adsorption sites for Hg [33, 34]. Li et al. [35] also suggested that oxygen surface complexes, possibly lactone (COO^-) and carbonyl (C=O) groups, are the potential sites for Hg capture.

Figure 3 shows the zeta potential of AC under different pH within 1–9. The zero point of charge of AC in Milli-Q water was shown to be around pH 1. Therefore, whether AC exists in natural environment or in the condition of this study (pH = 7), the surface charge of AC is always negative.

**Fig. 1** a The pore size distribution of AC based on NLDFT model and the SEM images of AC under b 40; c 200; and d 1500 x magnification

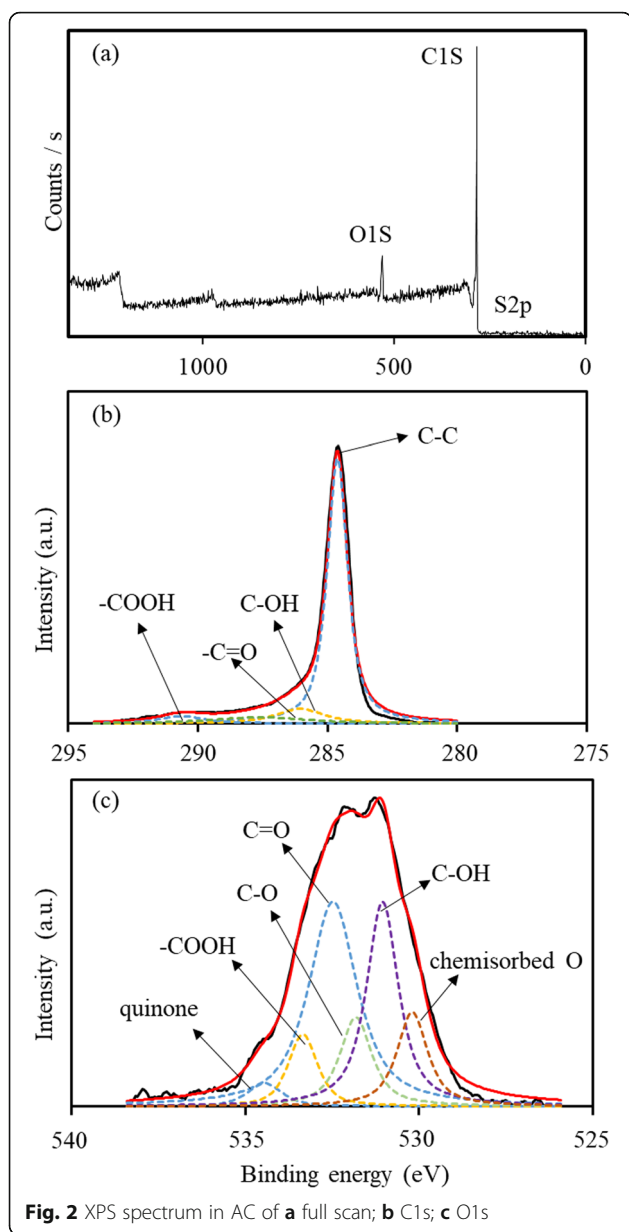


Fig. 2 XPS spectrum in AC of **a** full scan; **b** C1s; **c** O1s

Hg adsorption performance by AC

The AC dosage test was to determine the appropriate dosage for the batch experiments with a given initial Hg concentration. The past study showed that the contact time of Hg adsorption by AC was approximately 16 h to reach equilibrium [13]. To ensure reaching equilibrium, the contact time was set for 24 h in this part of batch experiments.

The initial Hg concentration was $18.4 \mu\text{g L}^{-1}$ under different AC dosages. The results of dosage test are listed in Table 2. This result shows that the increase in Hg removal efficiency and the decrease in adsorption capacity became less significant at the dosage from 50 to 80 mg. Therefore, 50 mg AC was considered as the suitable dosage for the following experiments in this study.

The Hg adsorption kinetics are different in the presence of chloride, sulfide, and DOM in the aqueous phase. Table 3 shows the test condition and the adsorption results under various contact time of Hg adsorption in the presence of chloride, sulfide, or DOM. Figure 4 further shows the residual dissolved Hg in the solution under various contact time up to 48 h. These experimental results suggest that the behaviors of Hg adsorption are significantly different in “Hg + Cl”, “Hg + sulfide”, and “Hg + DOM” conditions. To reach equilibrium, the contact time was at least 16, 10, and 24 h in “Hg + Cl”, “Hg + sulfide”, and “Hg + DOM” conditions, respectively. In order to further understand the possible Hg adsorption mechanisms, the adsorption kinetic models should be discussed. The equations of pseudo-first-order, pseudo-second order, and intraparticle diffusion model are given in Eqs. (3)–(5) and the fitting results are shown in Table 4.

$$\log(q_{e1} - q_t) = \log(q_{e1}) - \frac{k_1 t}{2.303} \quad (3)$$

$$\frac{t}{q_t} = \frac{1}{(k_2 \times q_{e2}^2)} + \frac{t}{q_{e2}} \quad (4)$$

$$q_t = k_p \times t^{0.5} + C \quad (5)$$

Data obtained in “Hg + Cl” condition had high R^2 (0.9998 and 0.9828) by pseudo-first order and pseudo-second order model fitting (Table 4). However, the calculated q_{e2} is more approximate to the experimental q_e . Data obtained in “Hg + sulfide” condition had a higher R^2 (0.9998) by pseudo-second order model fitting than R^2 (0.6886) by pseudo-first order model fitting. Data obtained in “Hg + DOM” condition had higher R^2 (0.9843) by pseudo-first order model fitting than R^2 (0.8503) by pseudo-second order model fitting. However, both the calculated q_{e1} and q_{e2} are similar to experimental q_e in “Hg + DOM” condition. Therefore, the Hg adsorption by AC in “Hg + Cl” and “Hg + DOM” conditions may follow both pseudo-first order and pseudo-second order reaction mechanisms. The fitting result for “Hg + DOM” condition was similar to Singh et al. [36], which reported that the adsorption of Hg interacted with organic ligands by kaolinite obeyed multiple first order kinetics. In the multiple first order kinetics adsorption process, they suggested that one stage corresponds to the initial binding with the active sites of the solid surface [37]. In this study, the reaction of Hg adsorption might be directly binding on AC with Hg-Cl and Hg-DOM complexes. However, the Hg adsorption reaction in “Hg + sulfide” condition was significantly different. The adsorption mechanism for “Hg + S” condition was more likely to fit pseudo-second order reaction based on the assumption that the rate-limiting step may be chemical adsorption

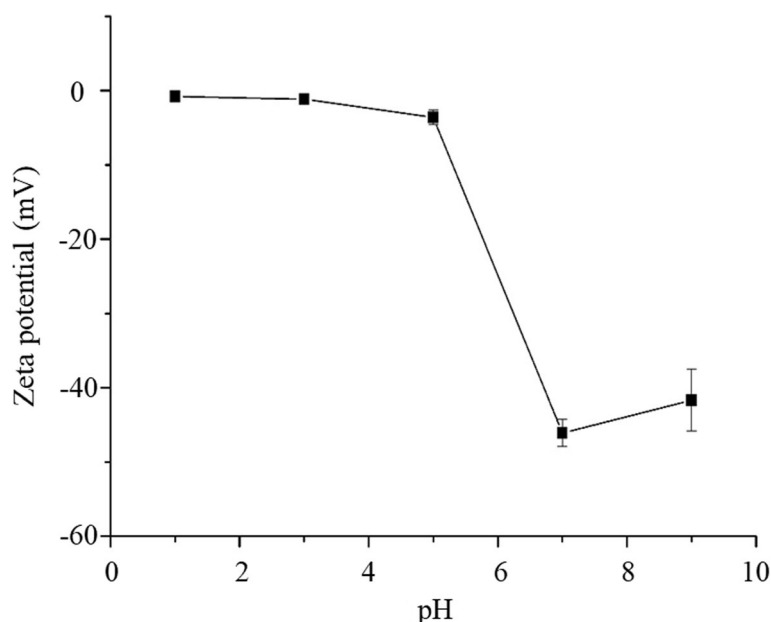


Fig. 3 Zeta potential of AC at different pH

or chemisorption involving valence forces through sharing or exchange of electrons [37]. Since a high affinity of sulfide bind to Hg, precipitation of Hg occurred in the adsorption process. The pseudo-first order rate constants k_1 for “Hg + Cl” and “Hg + DOM” were 0.0023 and 0.0009 min^{-1} respectively. The pseudo-second order rate constants k_2 for “Hg + Cl”, “Hg + S”, and “Hg + DOM” were 0.00057, 0.014 and 0.00022 $\text{g } \mu\text{g}^{-1} \text{min}^{-1}$. The additional sulfide promoted the reaction rate of Hg adsorption by AC due to the precipitation of HgS. Conversely, DOM decreased the Hg adsorption rate dramatically. Hg, a soft Lewis acid, has a strong affinity for thiol functional groups in DOM. Song et al. [27] reported that Hg interacting with natural organic matter had high thermodynamic stability. Past research has suggested that the complexation of Hg by DOM thiol groups could hinder nanoparticle β -HgS growth [38, 39]. For inference, the same mechanism could occur in the Hg + DOM adsorption by AC. DOM worked as a barrier to inhibit the contact of Hg with AC; therefore, adsorption in “Hg + DOM” condition had the lowest rate constant.

Table 2 The Hg adsorption results at various AC dosage

AC dosage (mg)	20	50	80
THg removal (%)	89	94	97
Adsorption capacity ($\mu\text{g g}^{-1}$)	42.9	18.2	11.6

Test liquid volume: 50 mL; initial Hg: 18.4 $\mu\text{g L}^{-1}$; pH: 6.98; dissolved O_2 : 4.27 mg L^{-1} ; shaking speed: 125 rpm; contact time: 24 h; temperature: 30 °C

The fitting results of intraparticle diffusion is also shown in Table 4. Data obtained in “Hg + Cl” and “Hg + DOM” condition had higher R^2 (0.9980 and 0.9508). Therefore, the Hg adsorption by AC in “Hg + Cl” and “Hg + DOM” conditions are more likely depended on intraparticle diffusion. The intraparticle diffusion rate constants k_p for “Hg + Cl” and “Hg + DOM” were 0.40 and 0.25 $\mu\text{g g}^{-1} \text{min}^{-0.5}$ respectively. The four basic steps of adsorption in a porous adsorbent included bulk solution transport, external transport, internal transport, and adsorption [40]. The AC used in this study is a porous adsorbent with high volume of micropores. The rate-limiting step in “Hg + Cl” and “Hg + DOM” is likely toward to intraparticle diffusion.

Table 3 The equilibrium results of Hg adsorption in the presence of chloride, sulfide, or DOM

	Hg + Cl	Hg + sulfide	Hg + DOM
Initial experimental parameters			
Hg conc. ($\mu\text{g L}^{-1}$)	16.2	18.6	20.4
Factor conc.	200 mM	10 μM	2 mg C L^{-1}
pH	6.86	6.76	6.96
Dissolved O_2 (mg L^{-1})	4.13	4.33	4.33
Contact time (min)	0–2880	0–1440	0–2880
After reaching equilibrium			
Residual dissolved THg ($\mu\text{g L}^{-1}$)	1.84	3.34	9.99
THg removal (%)	89	82	51
Adsorption capacity ($\mu\text{g g}^{-1}$)	14.3	15.3	10.4

The liquid volume: 50 mL; AC dosage: 50 mg; shaking speed: 125 rpm; temperature: 30 °C; contact time: 24 h

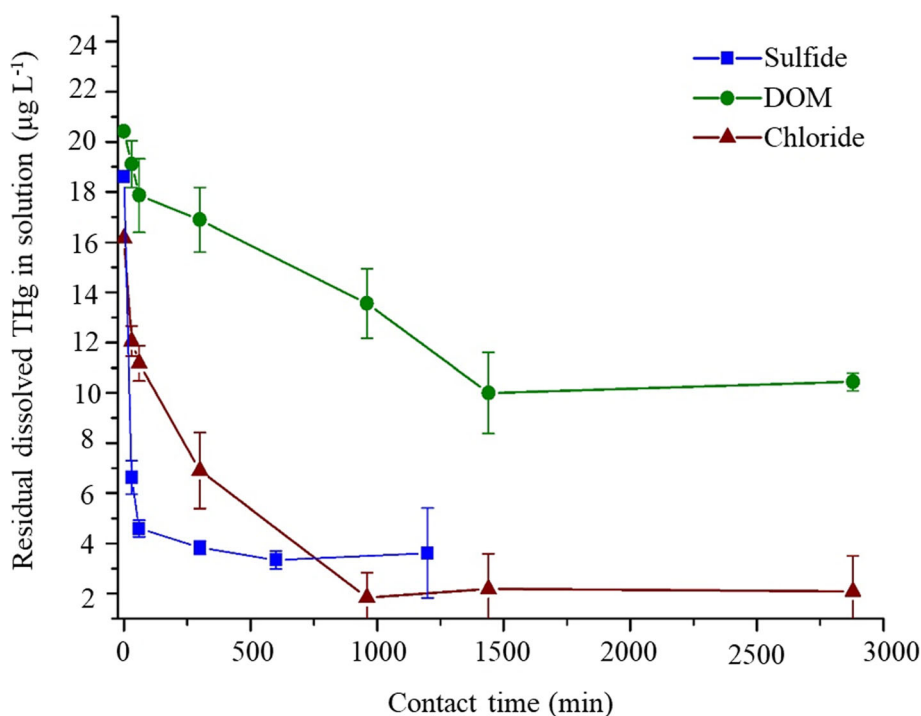


Fig. 4 The residual dissolved THg in solution under various contact time

Therefore, the adsorption rates are low in the “Hg + Cl” and “Hg + DOM” conditions.

Preliminary adsorption capacity comparison

Tables 2 and 3 show the adsorption capacity (q_e) of AC with and without additional chloride, sulfide, or DOM. The q_e in the absence of these environmental factors ($18.18 \mu\text{g g}^{-1}$) was slightly higher than the q_e in the “Hg + Cl” ($14.32 \mu\text{g g}^{-1}$) and “Hg + sulfide” ($15.26 \mu\text{g g}^{-1}$)

Table 4 The fitting results based on the pseudo-first, pseudo-second order and intraparticle diffusion kinetic models

	Hg + Cl	Hg + S	Hg + DOM
Pseudo first-order			
k_1 (min^{-1})	0.0023	0.0023	0.0009
q_{e1} ($\mu\text{g g}^{-1}$)	10.7	1.7	8.9
R^2	0.9998	0.6886	0.9843
Pseudo second-order			
k_2 ($\text{g } \mu\text{g}^{-1} \text{min}^{-1}$)	0.00057	0.014	0.00022
q_{e2} ($\mu\text{g g}^{-1}$)	16.1	15.4	11.6
R^2	0.9828	0.9998	0.8503
Intraparticle diffusion			
k_p ($\mu\text{g g}^{-1} \text{min}^{-0.5}$)	0.40	0.14	0.25
R^2	0.9980	0.7467	0.9508
Experimental q_e ($\mu\text{g g}^{-1}$)	14.3	15.3	10.4

conditions. AC in “Hg + DOM” condition had the lowest q_e ($10.4 \mu\text{g g}^{-1}$). In past studies, chloride interacting with Hg to form a stable complex was considered as the reason for decreasing the q_e of adsorbent [41, 42]. The additional sulfide seems to affect Hg adsorption on AC slightly. The DOM not only retarded Hg adsorption on AC but also decreased the q_e significantly. The more detailed discussion on these effects on q_e is presented in later section.

The calculation of q_e is generally done by measuring the Hg concentration changes in aqueous phase before and after AC adsorption. There was a doubt appeared that whether Hg actually adsorbed on AC or not because the q_e might be overestimated if Hg is reduced into Hg^0 and escaped into the air. Therefore, the investigation of Hg recovery by mass balance is necessary to ensure the accuracy of calculated q_e . In order to realize the influence of chloride on Hg adsorption, the recovery based on Hg mass balance before and after adsorption in the absence and presence of chloride had to be explored first (Fig. 5). The Hg recovery in the absence of chloride was 43%. The Hg recovery in the presence of chloride was 92%. Therefore, a various level of Hg could be escaped into the air in the absence of chloride. The reason for causing escape of Hg was due to the high pH value ($\text{pH} = 7$) of Hg solution. Chen et al. [43] reported that Hg^0 reemission rates from the wet flue gas desulfurization slurry increased about $4 \mu\text{g m}^{-3}$ as the pH values increased from 3 to 7; the Hg^0 reemission rate decreased

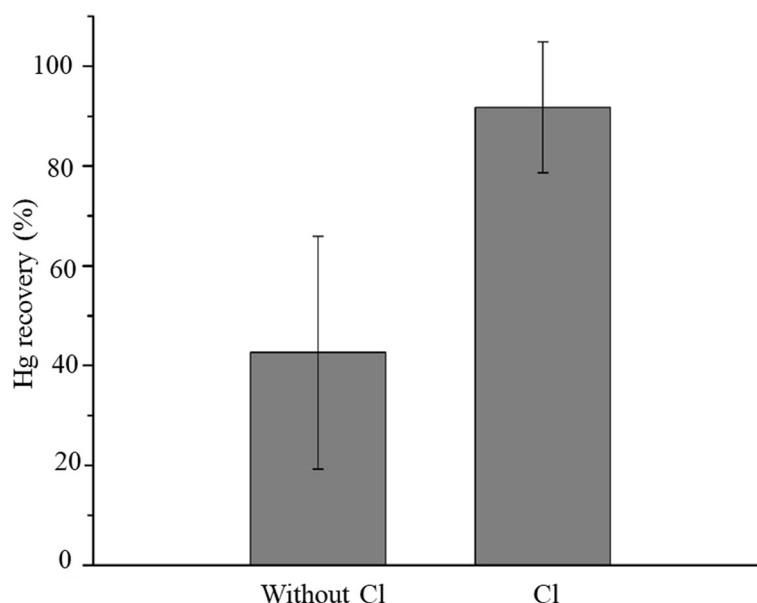


Fig. 5 Hg recovery test without and with chloride (200 mM). Initial Hg conc.: $19.3 \mu\text{g L}^{-1}$; volume: 50 mL; AC dosage: 0 mg; pH = 7; shaking speed: 125 rpm; temperature: 30°C ; contact time: 24 h

with increases chloride concentration. The acid condition could remain Hg^{2+} in the dissolved phase, as a result, Hg adsorption test was generally carried out under pH 3–5 [41, 44, 45]. However, the range of pH value is 6–8 in natural aquatic system. Therefore, it is reasonable to observe the apparent escape of Hg in this experimental condition (pH = 7). Nevertheless, adding chloride could enhance stabilizing Hg in the solution due to forming Hg-Cl complex. The phenomenon of Hg escaping into the air may thus possibly happen in this study as a result of the pH condition.

Hg distribution test results

The purpose of this part of the experiment is to realize the Hg distribution, including Hg in dissolved ($< 0.2 \mu\text{m}$) and solid phases ($> 0.2 \mu\text{m}$) under different concentration levels of sulfide/chloride/DOM. The test sample was divided into three parts including “dissolved Hg”, “particulate Hg”, and “Hg in AC”.

Hg + Cl⁻ condition

The “Hg + Cl⁻” test was carried out by conducting Hg adsorption by AC under the chloride concentration of 1, 200, and 400 mM. Table 5 describes the experimental parameters and the results of Hg distribution. The proportion of “dissolved Hg” under chloride concentration 1, 200, and 400 mM was calculated to be 2.7, 7.9, and 4.8%, respectively. The Hg removal efficiency was similar under the chloride concentration of 1, 200, and 400 mM and more than 90% of Hg was removed. The proportion of “Hg in AC” under chloride concentration 1, 200, and

400 mM was calculated to be 92.2, 99.5, and 93.6%, respectively. The particulate Hg was undetected in “Hg + Cl⁻” test. The Hg recovery (i.e., mass balance) in “Hg + Cl⁻” tests was calculated to be approximately 100% (i.e., 95–107%) (Table 5 and Fig. 6). Overall, the behavior of Hg adsorption on AC was nearly the same under the chloride concentration 1–400 mM.

The comparison of calculated q_e and THg removal efficiency between additional chloride concentration 0–400 mM is shown in Fig. 7. The THg removal efficiency was similar at the range of 92–95%. However, there was a significantly difference in calculated q_e . The q_e was 6.9, 13.8, 16.1, and $14.2 \mu\text{g g}^{-1}$ under the chloride concentration 0, 1, 200, and 400 mM, respectively. The reason may be an escape of Hg into the air in the absence of chloride. Therefore, the THg removal includes two mechanisms, Hg adsorbed in AC and Hg escaped to the gas phase in the absence of chloride. Practically, the increase in chloride concentration increased q_e due to the inhibition of Hg escape to the gas phase.

Past researches reported that the additional chloride decreased the Hg adsorption by AC or other relative adsorbents (Table S4). They suggested that Hg-Cl complex was a stable form and poorly adsorbed. Conversely, the presence of chloride could increase q_e in this study, which contradicted to previous studies. The reason might be the initial Hg concentrations in these studies were significantly different. The initial Hg concentration of previous studies was at the range of $10\text{--}50 \text{ mg L}^{-1}$; however, the Hg concentration was approximately $20 \mu\text{g L}^{-1}$ in this study. Therefore, the inhibition of Hg adsorption by chloride was

Table 5 Hg distribution under different chloride concentration

	Initial experimental parameters		
Chloride conc. (mM)	1	200	400
Hg conc. ($\mu\text{g L}^{-1}$)	14.3	16.2	15.2
pH	6.82	6.86	6.82
Dissolved O_2 (mg L^{-1})	3.97	3.83	4.40
	Hg partition after reaching equilibrium		
Dissolved Hg (%)	2.7	7.9	4.8
Hg in AC (%)	92.2	99.5	93.6
Particulate Hg (%)	0.02	nd	nd

The liquid volume: 50 mL; AC dosage: 50 mg; shaking speed: 125 rpm; temperature: 30 °C; contact time: 24 h

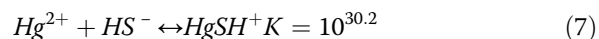
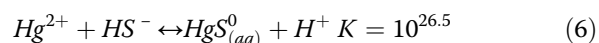
not obvious in our results. The second possible reason could be an overestimate of q_e in the previous studies. There was a doubt of Hg escaping into the air in the absence of chloride or in high pH condition [43]. Nevertheless, the calculation method of q_e was typically based on the difference in initial and residual Hg concentrations in previous studies. Additionally, the Hg recovery test was not conducted in these relative studies. Therefore, overestimated q_e probably occurred in previous studies.

“Hg + sulfide” condition

The “Hg + sulfide” test was carried out by Hg adsorption on AC under sulfide concentrations of 2, 10, and 20 μM . Table 6 describes the experimental parameters and the results of Hg distribution. The proportion of “dissolved

Hg” under sulfide concentration 2, 10, and 20 μM was 25.2, 35.1, and 25.0%, respectively; the proportion of “Hg in AC” was 28.7, 33.1, and 28.1%, respectively; and the proportion of “particulate Hg” was 28.7, 26.8, and 23.6%, respectively (Fig. 8).

Sulfide has a strong affinity for Hg tending to form Hg-S (Eq. (6)) [23]. During an aging process, Hg-S aggregated into large particulate form of HgS [21, 26, 46]. Through 24 h contacting with sulfide, there was an amount of Hg forming into particles ($>0.2 \mu\text{m}$) in this study. The initial Hg concentration was around 20 $\mu\text{g L}^{-1}$ (0.1 μM); however, sulfide concentrations (2, 10, and 20 μM) were at least 20 times higher than Hg concentration. Therefore, sulfide concentration was greatly in excess than the stoichiometric value based on Eqs. (6) and (7). Consequently, a certain proportion of particulate Hg would be formed. The Hg recovery was around 80% in “Hg + S” condition, which may be partly due to experimental error because the sample of 5 mL was firstly taken for measuring “dissolved Hg” that may cause particulate Hg loss.



Around 30% of Hg was adsorbed on AC under different sulfide concentrations. A portion of Hg was formed as HgSH⁺ in “Hg + S” (Eq. (7)). The surface charge of AC was negative in this condition (Fig. 3). Therefore, the Hg species tended to be adsorbed on AC by Van der

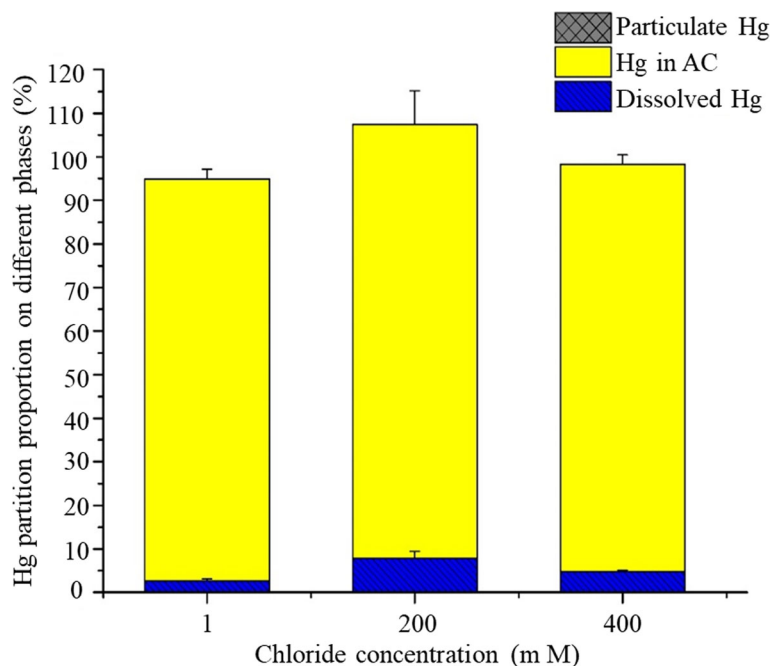
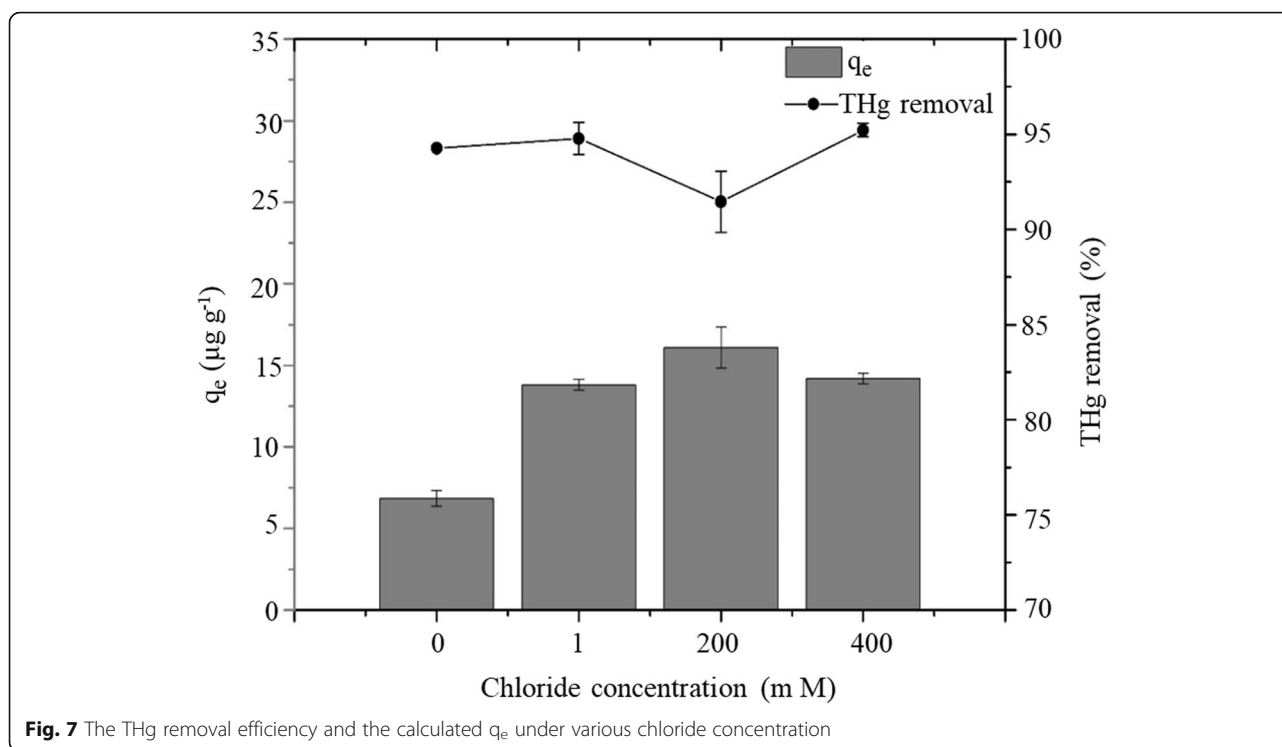


Fig. 6 Hg partition proportion on different phases under different chloride concentration



Wall's force. Moreover, data from "Hg + S" test can be well fitted to the pseudo-second order model. There were two possible mechanisms to remove Hg. One of the mechanisms was chemical precipitation by Hg bonded to sulfide to form $HgS_{(s)}$. The other was adsorption of $HgSH^+$ by AC. Furthermore, a portion of Hg might exist in the form of $HgS_{(aq)}$ which was poorly adsorbed by AC. Therefore, the proportion of "dissolved Hg" in "Hg + S" (around 25%) was higher than in "Hg + Cl" (around 5%).

"Hg + DOM" condition

The "Hg + DOM" test was carried out by Hg adsorption on AC under various DOM concentration within 0.25–20 $mg\ C\ L^{-1}$. Table 7 describes the experimental parameters and the results of Hg distribution. The proportion of

"dissolved Hg" under DOM concentration 0.25, 0.5, 2, 10, and 20 $mg\ C\ L^{-1}$ was 45.1, 57.8, 61.4, 68.4, and 75.7% respectively; the proportion of "Hg in AC" was 61.5, 49.3, 49.1, 26.9, and 14.7% respectively; and the proportion of "particulate Hg" was 3.1, 4.6, 3.2, 2.5, and 2.1% respectively.

Figure 9 further shows that increasing DOM concentration resulted in more dissolved phase of Hg in the solution. The proportion of "dissolved Hg" increased 30.6% from DOM concentration 0.25 to 20 $mg\ C\ L^{-1}$. This result was also reflected in "Hg in AC". The proportion of "Hg in AC" decreased by 46.8% from DOM concentration 0.25 to 20 $mg\ C\ L^{-1}$. The reason for inhibition of Hg adsorption may be due to the affinity of DOM for Hg. The elemental compositions of SRHA are listed in Table S5. Graham et al. [47] reported that the reduced sulfur in SRHA is about 18.3 mol% of total sulfur. Therefore, the ratio of C to reduced sulfur is 542 (w/w). Xia et al. [48] reported that reduced S in SRHA analyzed by XANES was in the form of thiol/sulfide and thiophene. The thiol functional group on DOM was the major binding site with Hg [27, 28]. Among the ligands, sulfur-containing ligands bind Hg much more strongly than oxygen-containing ligands, which appear in AC [28]. Therefore, the phenomenon of Hg escaping is not apparent and the recovery of Hg is approximately 100% (Fig. 9). In addition to thiol functional group, DOM also contained carboxyl (about 9 $meq\ g^{-1}\ C$) and phenolic (about 4 $meq\ g^{-1}\ C$) functional groups, which are effective binding sites for Hg

Table 6 Hg distribution under different sulfide concentration

	Initial experimental parameters		
Sulfide conc. (μM)	2	10	20
Hg conc. ($\mu g\ L^{-1}$)	16.61	17.53	18.60
pH	6.83	7.43	6.96
Dissolved O_2 ($mg\ L^{-1}$)	3.99	3.30	4.22
	Hg partition after reaching equilibrium		
Dissolved Hg (%)	25.2	35.1	25.0
Hg in AC (%)	28.7	33.1	28.1
Particulate Hg (%)	28.7	26.8	23.6

The liquid volume: 50 mL; AC dosage: 50 mg; shaking speed: 125 rpm; temperature: 30 °C; contact time: 24 h

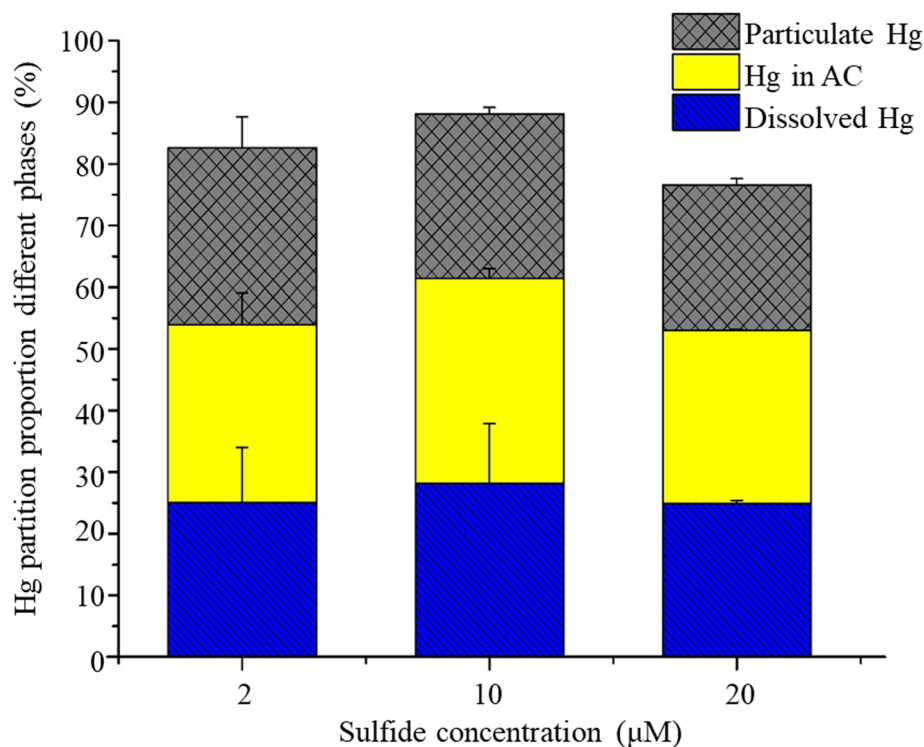


Fig. 8 Hg partition proportion on different phases under different sulfide concentration

[33, 34]. Hence, DOM is a large molecule tending to bind to Hg. This kind of molecule (DOM-Hg) then separated Hg from adsorption on AC. Since AC is usually nonpolar or slightly polar, DOM was considered as a stabilization agent for Hg instead of a carrier for Hg adsorption onto AC. Therefore, the DOM increased concentration may inhibit Hg adsorption dramatically.

In addition to DOM stabilizing Hg in dissolved phase, the formation of β -HgS particles from Hg^{2+} interacting with DOM was found in others [49, 50]. The particle size of β -HgS nanoparticles was around 3–5 nm reported by Manceau et al. [50]. Therefore, β -HgS nanoparticles

might be formed in this study. If the particle size of β -HgS was lower than 0.2 μm , it would be classified into “dissolved Hg” in this study. The formation of β -HgS nanoparticles was also a reason for increasing the proportion of “dissolved Hg”. However, β -HgS nanoparticles had the ability of aggregation. Therefore, even with the presence of DOM, β -HgS particles (> 0.2 μm) might still be formed during the adsorption process with a 24-h duration. For here, 2.1–4.6% of Hg particles were formed in “Hg + DOM”. This result showed that DOM could inhibit β -HgS aggregation significantly in this study.

Conclusions

The main aim of this study is to better understand the influences of chloride, sulfide, and DOM concentrations on the Hg adsorption equilibrium and kinetics of AC in an aqueous system. The important findings in this study are concluded as follows:

1. The rate of Hg adsorption on AC varied with the presence of sulfide, chloride, and DOM, from fast to slow. Hg adsorption might be directly bonded on AC with Hg-Cl and Hg-DOM complexes. The Hg adsorption kinetics by AC in “Hg + Cl” and “Hg + DOM” conditions are mainly controlled by intraparticle diffusion. Data from “Hg + S” test were better fitted to pseudo-second order model, resulting from

Table 7 Hg distribution under different DOM concentration

	Initial experimental parameters				
	0.25	0.5	2	10	20
DOM conc. (mg C L^{-1})	0.25	0.5	2	10	20
Hg conc. ($\mu\text{g L}^{-1}$)	18.0	12.4	12.1	13.9	15.9
pH	6.73	6.94	6.87	6.86	6.94
Dissolved O_2 (mg L^{-1})	4.33	3.71	3.65	3.67	3.13
	Hg partition after reaching equilibrium				
Dissolved Hg (%)	45.1	57.8	61.4	68.4	75.7
Hg in AC (%)	61.5	49.3	49.1	26.9	14.7
Particulate Hg (%)	3.1	4.6	3.2	2.5	2.1

The liquid volume: 50 mL; AC dosage: 50 mg; shaking speed: 125 rpm; temperature: 30 $^{\circ}\text{C}$; contact time: 24 h

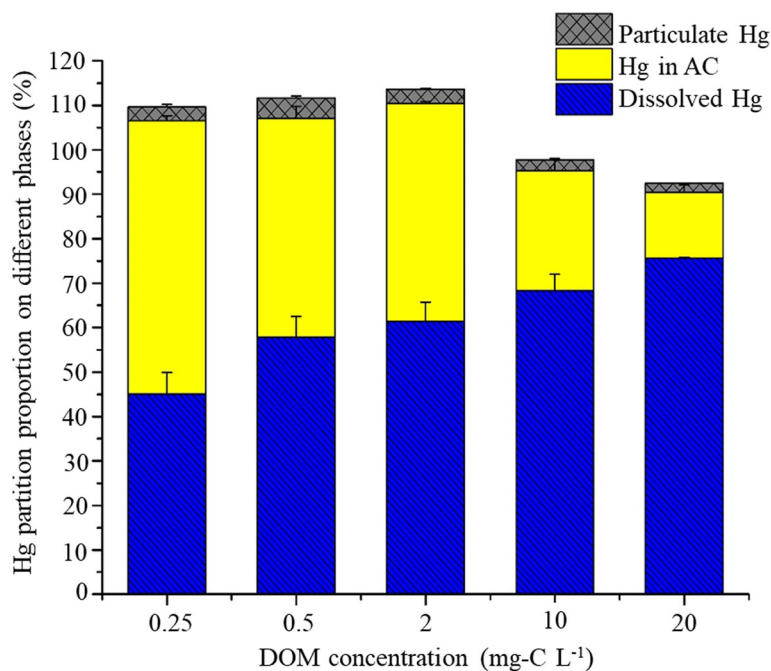


Fig. 9 Hg partition proportion on different phases under different DOM concentration

Hg adsorption into AC and chemisorption of sulfide and Hg.

- There were various levels of Hg escaping into the air in the absence of chloride in this study. Therefore, the investigation of Hg distribution is necessary to ensure the accuracy of calculated equilibrium capacity (q_e) by mass balance, which could be overestimated by several earlier studies.
- The THg removal efficiency (92–95%) was similar in the absence and the presence of chloride (1–400 mM). The increase in chloride concentration practically increased the q_e due to inhibition of Hg escape in this study. This result was different with those of previous studies, which may be due to the significant difference in initial Hg concentration and the overestimated q_e in past studies.
- The THg removal efficiency was around 65–75% in “Hg + sulfide” test. Among the removed Hg, there were 24–29% of Hg forming into particles and around 30% of Hg adsorbed on AC under sulfide concentration (2–20 μM). Hg of 25–35% might exist in the form of $\text{HgS}_{(\text{aq})}$ which was hardly adsorbed by AC.
- Increasing DOM concentration led to more dissolved phase of Hg in “Hg + DOM” condition. The proportion of “dissolved Hg” increased 31% from DOM concentration 0.25 to 20 mg C L^{-1} . Simultaneously, the proportion of “Hg in AC” decreased 47%. Thiol groups on DOM binding with

Hg could separate Hg from the adsorption phase of AC and stabilize Hg in the dissolved phase.

- Overall, the presence of Cl^- increased the Hg adsorption on AC. It is a positive effect for AC application in thin layer capping. However, sulfide and DOM significantly decreased q_e due to the formation of Hg-S and Hg-DOM. In particular, the negative effect of DOM should be overcome in future application.

Supplementary information

Supplementary information accompanies this paper at <https://doi.org/10.1186/s42834-020-00065-5>.

Additional file 1.

Acknowledgements

This work was financially supported by the Environmental Protection Administration, Taiwan under Grant no. 107c000734. The opinions expressed in this paper are not necessarily those of the sponsor.

Authors' contributions

Conceptualization, C.C., Y.T., and H.C.H.; methodology, C.C., Y.T., and B.L.C.; formal analysis, C.C.; investigation, C.C.; data curation, C.C.; writing—original draft preparation, C.C. and H.C.H.; writing—review and editing, H.C.H.; visualization, C.C.; funding acquisition, H.C.H. All authors read and approved the final manuscript.

Funding

This work was financially supported by the Environmental Protection Administration, Taiwan under Grant no. 107c000734.

Availability of data and materials

All data generated or analyzed during this study are included in this published article and its supplementary information files.

Competing interests

The authors declare they have no competing interests.

Received: 14 June 2020 Accepted: 11 September 2020

Published online: 29 September 2020

References

- Hong YS, Kim YM, Lee KE. Methylmercury exposure and health effects. *J Prev Med Public Health*. 2012;45:353–63.
- Carocci A, Rovito N, Sinicropi MS, Genchi G. Mercury toxicity and neurodegenerative effects. In: Whitacre DM, editor. *Reviews of environmental contamination and toxicology*. Volume 229. Cham: Springer; 2014. p. 1–18.
- Bailey LT, Mitchell CPJ, Engstrom DR, Berndt ME, Wasik JKC, Johnson NW. Influence of porewater sulfide on methylmercury production and partitioning in sulfate-impacted lake sediments. *Sci Total Environ*. 2017;580:1197–204.
- UNEP. *Global Mercury Assessment 2013: Sources, Emissions, Releases and Environmental Transport*. Geneva: UNEP Chemicals Branch; 2013.
- Gilmour CC, Podar M, Bullock AL, Graham AM, Brown SD, Somenahally AC, et al. Mercury methylation by novel microorganisms from new environments. *Environ Sci Technol*. 2013;47:11810–20.
- Wang YL, Fang MD, Chien LC, Lin CC, Hsi HC. Distribution of mercury and methylmercury in surface water and surface sediment of river, irrigation canal, reservoir, and wetland in Taiwan. *Environ Sci Pollut R*. 2019;26:17762–73.
- Ghosh U, Luthy RG, Cornelissen G, Werner D, Menzie CA. In-situ sorbent amendments: a new direction in contaminated sediment management. *Environ Sci Technol*. 2011;45:1163–8.
- Randall PM, Chattopadhyay S. Mercury contaminated sediment sites – an evaluation of remedial options. *Environ Res*. 2013;125:131–49.
- Rudd J, Harris R, Sellers P. *Advice on Mercury Remediation Options for the Wabigoon-English River System*. 2016.
- Kupryianchuk D, Rakowska M, Reible D, Harmsen J, Cornelissen G, van Veggel M, et al. Positioning activated carbon amendment technologies in a novel framework for sediment management. *Integr Environ Asses*. 2015;11:221–34.
- Martins M, Costa PM, Raimundo J, Vale C, Ferreira AM, Costa MH. Impact of remobilized contaminants in *Mytilus edulis* during dredging operations in a harbour area: bioaccumulation and biomarker responses. *Ecotox Environ Safe*. 2012;85:96–103.
- Zhang C, Zhu MY, Zeng GM, Yu ZG, Cui F, Yang ZZ, et al. Active capping technology: a new environmental remediation of contaminated sediment. *Environ Sci Pollut R*. 2016;23:4370–86.
- Ting Y, Chen C, Ch'ng BL, Wang YL, Hsi HC. Using raw and sulfur-impregnated activated carbon as active cap for leaching inhibition of mercury and methylmercury from contaminated sediment. *J Hazard Mater*. 2018;354:116–24.
- Ting Y, Hsi HC. Iron sulfide minerals as potential active capping materials for mercury-contaminated sediment remediation: a minireview. *Sustainability-Basel*. 2019;11:1747.
- Saha B, Tai MH, Streat M. Study of activated carbon after oxidation and subsequent treatment characterization. *Process Saf Environ*. 2001;79:211–7.
- Lu XC, Jiang JC, Sun K, Xie XP, Hu YM. Surface modification, characterization and adsorptive properties of a coconut activated carbon. *Appl Surf Sci*. 2012;258:8247–52.
- Lu XC, Jiang JC, Sun K, Wang JB, Zhang YP. Influence of the pore structure and surface chemical properties of activated carbon on the adsorption of mercury from aqueous solutions. *Mar Pollut Bull*. 2014;78:69–76.
- Hsu CJ, Chiou HJ, Chen YH, Lin KS, Rood MJ, Hsi HC. Mercury adsorption and re-emission inhibition from actual WFGD wastewater using sulfur-containing activated carbon. *Environ Res*. 2019;168:319–28.
- Hsu CJ, Chen YH, Hsi HC. Adsorption of aqueous Hg^{2+} and inhibition of Hg^0 re-emission from actual seawater flue gas desulfurization wastewater by using sulfurized activated carbon and $NaClO$. *Sci Total Environ*. 2020;711:135172.
- Rickards D, Mussmann M, Steadman JA. Sedimentary sulfides. *Elements*. 2017;13:117–22.
- Mazrui NM, Jonsson S, Thota S, Zhao J, Mason RP. Enhanced availability of mercury bound to dissolved organic matter for methylation in marine sediments. *Geochim Cosmochim Acta*. 2016;194:153–62.
- Jonsson S, Skyllberg U, Nilsson MB, Westlund PO, Shchukarev A, Lundberg E, et al. Mercury methylation rates for geochemically relevant Hg^I species in sediments. *Environ Sci Technol*. 2012;46:11653–9.
- Benoit JM, Mason RP, Gilmour CC. Estimation of mercury-sulfide speciation in sediment pore waters using octanol–water partitioning and implications for availability to methylating bacteria. *Environ Toxicol Chem*. 1999;18:2138–41.
- Deonarine A, Hsu-Kim H. Precipitation of mercuric sulfide nanoparticles in NOM-containing water: implications for the natural environment. *Environ Sci Technol*. 2009;43:2368–73.
- Findlay SEG, Parr TB. Dissolved organic matter. In: Lamberti GA, Hauer FR, editors. *Methods in stream ecology*. 3rd ed. Volume 2: ecosystem function. London: Academic Press; 2017. p. 21–36.
- Mazrui NM, Seelen E, King'ondo CK, Thota S, Awino J, Rouge J, et al. The precipitation, growth and stability of mercury sulfide nanoparticles formed in the presence of marine dissolved organic matter. *Environ Sci-Proc Imp*. 2018;20:642–56.
- Song Y, Jiang T, Liem-Nguyen V, Sparrman T, Bjorn E, Skyllberg U. Thermodynamics of Hg (II) bonding to thiol groups in Suwannee River natural organic matter resolved by competitive ligand exchange, Hg_{LIII} -edge EXAFS and 1H NMR spectroscopy. *Environ Sci Technol*. 2018;52:8292–301.
- Ravichandran M. Interactions between mercury and dissolved organic matter – a review. *Chemosphere*. 2004;55:319–31.
- Lee S, Roh Y, Kim KW. Influence of chloride ions on the reduction of mercury species in the presence of dissolved organic matter. *Environ Geochem Hlth*. 2019;41:71–9.
- Hsi HC, Rood MJ, Rostam-Abadi M, Chen SG, Chang R. Effects of sulfur impregnation temperature on the properties and mercury adsorption capacities of activated carbon fibers (ACFs). *Environ Sci Technol*. 2001;35:2785–91.
- Martinez MT, Callejas MA, Benito AM, Cochet M, Seeger T, Anson A, et al. Sensitivity of single wall carbon nanotubes to oxidative processing: structural modification, intercalation and functionalisation. *Carbon*. 2003;41:2247–56.
- Oh YJ, Yoo JJ, Kim YI, Yoon JK, Yoon HN, Kim JH, et al. Oxygen functional groups and electrochemical capacitive behavior of incompletely reduced graphene oxides as a thin-film electrode of supercapacitor. *Electrochim Acta*. 2014;116:118–28.
- Faheem, Bao JG, Zheng H, Tufail H, Irshad S, Du JK. Adsorption-assisted decontamination of Hg (II) from aqueous solution by multi-functionalized corn-cob-derived biochar. *RSC Adv*. 2018;8:38425–35.
- Dong XL, Ma LNQ, Zhu YJ, Li YC, Gu BH. Mechanistic investigation of mercury sorption by Brazilian pepper biochars of different pyrolytic temperatures based on X-ray photoelectron spectroscopy and flow calorimetry. *Environ Sci Technol*. 2013;47:12156–64.
- Li YH, Lee CW, Gullett BK. Importance of activated carbon's oxygen surface functional groups on elemental mercury adsorption. *Fuel*. 2003;82:451–7.
- Singh J, Huang PM, Hammer UT, Liaw WK. Influence of citric acid and glycine on the adsorption of mercury (II) by kaolinite under various pH conditions. *Clay Clay Miner*. 1996;44:41–8.
- Ho YS, McKay G. Pseudo-second order model for sorption processes. *Process Biochem*. 1999;34:451–65.
- Poulin BA, Gerbig CA, Kim CS, Stegemeier JP, Ryan JN, Aiken GR. Effects of sulfide concentration and dissolved organic matter characteristics on the structure of nanocolloidal metacinnabar. *Environ Sci Technol*. 2017;51:13133–42.
- Aiken GR, Hsu-Kim H, Ryan JN. Influence of dissolved organic matter on the environmental fate of metals, nanoparticles, and colloids. *Environ Sci Technol*. 2011;45:3196–201.
- Asasian N, Kaghazchi T, Soleimani M. Elimination of mercury by adsorption onto activated carbon prepared from the biomass material. *J Ind Eng Chem*. 2012;18:283–9.
- Boutsika LG, Karapanagioti HK, Manariotis ID. Effect of chloride and nitrate salts on Hg (II) sorption by raw and pyrolyzed malt spent rootlets. *J Chem Technol Biot*. 2017;92:1912–8.

42. Robles I, Bustos E, Lakatos J. Adsorption study of mercury on lignite in the presence of different anions. *Sustain Environ Res*. 2016;26:136–41.
43. Chen CM, Liu ST, Gao Y, Liu YC. Investigation on mercury reemission from limestone-gypsum wet flue gas desulfurization slurry. *Sci World J*. 2014;2014: 581724.
44. Ranganathan K. Adsorption of Hg (II) ions from aqueous chloride solutions using powdered activated carbons. *Carbon*. 2003;41:1087–92.
45. Namasivayam C, Kadirvelu K. Uptake of mercury (II) from wastewater by activated carbon from an unwanted agricultural solid by-product: coirpith. *Carbon*. 1999;37:79–84.
46. Pham ALT, Morris A, Zhang T, Ticknor J, Levard C, Hsu-Kim H. Precipitation of nanoscale mercuric sulfides in the presence of natural organic matter: structural properties, aggregation, and biotransformation. *Geochim Cosmochim Acta*. 2014;133:204–15.
47. Graham AM, Aiken GR, Gilmour CC. Dissolved organic matter enhances microbial mercury methylation under sulfidic conditions. *Environ Sci Technol*. 2012;46:2715–23.
48. Xia K, Weesner F, Bleam WF, Bloom PR, Skjellberg UL, Helmke PA. XANES studies of oxidation states of sulfur in aquatic and soil humic substances. *Soil Sci Soc Am J*. 1998;62:1240–6.
49. Luo HW, Yin XP, Jubbb AM, Chen HM, Lu X, Zhang WH, et al. Photochemical reactions between mercury (Hg) and dissolved organic matter decrease Hg bioavailability and methylation. *Environ Pollut*. 2017;220:1359–65.
50. Manceau A, Lemouchi C, Enescu M, Gaillot AC, Lanson M, Magnin V, et al. Formation of mercury sulfide from Hg (II)-thiolate complexes in natural organic matter. *Environ Sci Technol*. 2015;49:9787–96.

Publisher's Note

Springer Nature remains neutral with regard to jurisdictional claims in published maps and institutional affiliations.

Ready to submit your research? Choose BMC and benefit from:

- fast, convenient online submission
- thorough peer review by experienced researchers in your field
- rapid publication on acceptance
- support for research data, including large and complex data types
- gold Open Access which fosters wider collaboration and increased citations
- maximum visibility for your research: over 100M website views per year

At BMC, research is always in progress.

Learn more biomedcentral.com/submissions

